Theory of solid-state contributions to the x-ray elastic scattering amplitude

A. L. Ankudinov and J. J. Rehr
Deptartment of Physics, University of Washington, Seattle, Washington 98195-1560
(Received 1 February 2000)

We present a real space Green's function theory of solid-state contributions and polarization dependence of the x-ray elastic scattering amplitude. In this approach the calculation separates naturally into contributions from the central (embedded) absorbing atom and multiple-scattering contributions from the environment. Both real and imaginary parts of the anomalous x-ray scattering amplitude are calculated simultaneously in the complex energy plane, without the necessity of a Kramers-Kronig transform. This approach also takes into account final-state effects, including core-hole lifetime, the finite temperature Fermi distribution and Debye-Waller factors, as well as experimental resolution. The approach is implemented in a generalization of the *ab initio*, self-consistent code, FEFF8.10, which permits applications to a number of x-ray spectroscopies for general, not necessarily periodic systems. The solid-state effect on the fine structure in the anomalous scattering amplitude near an absorption edge is illustrated for Cu metal. Calculations are also presented of the x-ray anomalous cross scattering amplitude $F_{\pi\sigma}$ for Cd metal, and x-ray natural circular dichroism in $LiIO_3$, which are both due entirely to solid-state effects.

I. INTRODUCTION

Knowledge of x-ray scattering amplitudes in matter is important for many applications, e.g., for the analysis of x-ray diffraction data, anomalous x-ray scattering experiments, etc. Remarkably, most of the available calculations of such scattering amplitudes, e.g., the widely used tables of Cromer and Liberman[1] and other more recent approaches,[2] are based on purely atomic models. However, for photon energies above an absorption edge, solid-state effects lead to an oscillatory fine structure in the anomalous x-ray scattering amplitude $f'+if''$, due to the photoelectron scattering by the environment of the central atom. This structure[3] is directly analogous to the phenomenon of x-ray absorption fine structure (XAFS), and hence can be calculated with similar techniques. Thus the amplitude of the solid-state effect on f' is typically about 0.5 or more electron units, i.e., about 10–20%, and cannot be neglected. For studies of multielement compounds, such as biological materials, these effects are especially important, as it could be difficult to avoid the near edge region in scattering experiments. Moreover, several related experimental techniques, such as diffraction anomalous fine structure (DAFS) and x-ray reflectivity fine structure,[4,5] are based on the analysis of the oscillatory structure. As in x-ray absorption, this signal contains information about the geometry of neighboring scatterers, but can be more site or surface specific. For example, by using DAFS, Cross *et al.* were able to separate the local environments of two nonequivalent Cu sites in high-temperature superconductors.[3] To analyze this fine structure for structural studies it is essential to know both real and imaginary parts of the elastic-scattering amplitude, including solid-state effects.

One way to calculate the solid-state effect in x-ray scattering is to use a differential Kramers-Kronig (DKK) transform[3] for the real part of the x-ray scattering amplitude, starting from calculations of the x-ray absorption coefficient, which is proportional to the imaginary part f''. Unfortunately the DKK method requires *a priori* knowledge of the very high-energy behavior of the anomalous scattering amplitude f', which requires separate calculations or measurements. The method is also expected to have difficulty for low-symmetry crystals, where the real and imaginary parts of scattering amplitudes cannot be diagonalized simultaneously, and when quadrupole transitions play an important role.

To avoid these difficulties here, we make use of a real space Green's function (RSGF) formalism[6] to develop a theory that is applicable for any symmetry and that also includes multipole transitions and cross terms. In this approach, both real and imaginary parts of the full complex x-ray scattering amplitude $f=f^T+f'+if''$ are calculated simultaneously by real-space multiple-scattering (MS) calculations in the complex energy plane, without the necessity of the DKK transform, where f^T is the Thomson scattering amplitude. The complex plane approach permits a proper treatment of the finite temperature Fermi distribution as well as final-state effects such as core-hole lifetime and experimental resolution. The theory is implemented in a generalization of the self-consistent x-ray spectroscopy code[6] FEFF8 (version 8.10), which is applicable to a number of x-ray spectroscopies. This generalization also extends the capabilities of FEFF8 for absorption spectra, permitting higher excited-state energies and an improved treatment of the edge shape and atomic background[7] due to a proper subtraction of contributions from occupied states. We illustrate the solid-state effects with FEFF8.10 calculations of the x-ray anomalous scattering amplitude f', the x-ray anomalous scattering cross term (XACS) $F_{\pi\sigma}$, and x-ray natural circular dichroism (XNCD) due to dipole-quadrupole scattering. All of these calculations are found to be in good agreement with experimental data.

II. THEORY

The x-ray elastic-scattering amplitude can naturally be separated into Rayleigh scattering (which includes both Thomson and anomalous x-ray scattering contributions), nuclear Thomson ($f^{NT}=r_0Z^2m/M_{at}$) and Delbrück

scattering,[2,8] where Z is the atomic number, $r_0=e^2/mc^2$ is the classical radius of the electron, m the electron mass, and M_{at} the atomic mass (unless otherwise specified, we use atomic units $e=m=\hbar=1$ throughout this paper). The last two contributions are important for γ rays, but in the x-ray regime (photon energy less than 60 keV), which is of primary interest in this paper, they can be neglected. Thus, starting from the relativistic quantum electrodynamics expression for the Rayleigh scattering amplitude in traditional electron units (i.e. in units of the classical electron radius ''$-r_0$'')

$$\frac{f(\omega,\vec{k}',\hat{\epsilon}',\vec{k},\hat{\epsilon})}{mc^2}=\sum_F^{\text{all}}\frac{\langle I|(\hat{\epsilon}'\cdot\vec{\alpha})^\dagger e^{-i\vec{k}'\cdot\vec{r}}|F\rangle\langle F|\hat{\epsilon}\cdot\vec{\alpha}e^{i\vec{k}\cdot\vec{r}}|I\rangle}{E_I-E_F+\hbar\omega+i\Gamma_F}+\frac{\langle I|(\hat{\epsilon}\cdot\vec{\alpha})^\dagger e^{-i\vec{k}\cdot\vec{r}}|F\rangle\langle F|\hat{\epsilon}'\cdot\vec{\alpha}e^{i\vec{k}'\cdot\vec{r}}|I\rangle}{E_I-E_F-\hbar\omega-i\Gamma_F}, \tag{1}$$

where I and F are the many-body initial and final states of the system. The forward-scattering amplitude (FSA) $f_{\alpha\beta}(\omega)$ for $\vec{k}=\vec{k}'$ is particularly interesting due to its connection with the dielectric tensor[9,10] $\epsilon_{\alpha\beta}(\omega)$,

$$\epsilon_{\alpha\beta}(\omega)=\delta_{\alpha\beta}+4\pi\chi_{\alpha\beta}(\omega),$$

$$\chi_{\alpha\beta}(\omega)=\frac{-r_0}{vk^2}\sum_i f_{\alpha\beta}(\omega), \tag{2}$$

where $k=\omega/c$ is the photon wave vector, v is volume of the unit cell in a crystalline material or the volume per molecule in gases and liquids, and the sum goes over the atoms in the unit cell or the molecule, respectively. This connection shows that knowledge of the microscopic quantity (FSA) is sufficient to obtain the index of refraction, Kerr effect, and other macroscopic response functions. Within the independent electron approximation one obtains, after performing a summation over negative-energy states[1,8]

$$f(\omega,\vec{k}',\hat{\epsilon}',\vec{k},\hat{\epsilon})=(\hat{\epsilon}'^*\cdot\hat{\epsilon})[g(Q)+f^{ss}(\vec{Q})]+\sum_{p,p'=\pm1}(\epsilon'_{-p'})^*[f^A_{p'p}+\overline{f}^A_{p',p}]\epsilon_{-p}, \tag{3}$$

$$g(Q)=\sum_j\int r^2dr\rho_j^{at}(r)\frac{\sin(Qr)}{Qr}\frac{mc^2}{E_j-V(r)},$$

$$f^{ss}(\vec{Q})=\int d^3r\,\delta\rho(\vec{r})e^{-i\vec{Q}\cdot\vec{r}},$$

$$\frac{f^A_{p'p}(\omega,\vec{k}',\vec{k})}{mc^2}=\sum_j^{occ}\sum_f^{unocc}\frac{\langle i|\alpha^\dagger_{p'}e^{-i\vec{k}'\cdot\vec{r}}|f\rangle\langle f|\alpha_p e^{i\vec{k}\cdot\vec{r}}|i\rangle}{E_j-E_f+\hbar\omega+i\Gamma_j},$$

$$\overline{f}^A_{p'p}(\omega,\vec{k}',\vec{k})=[f^A_{-p',-p}(-\omega,-\vec{k}',-\vec{k})]^*.$$

The above expressions are written in circular polarization notation (cf. Messiah,[11] pp. 1034–1036), which simplifies the angular momentum algebra in the calculations. The natural Cartesian frames of reference are different for initial and final multipole matrix elements. It is convenient to choose $\hat{z}$ along $\vec{k}$, $\hat{z}'$ along $\vec{k}'$ and the same y axis along $\vec{k}\times\vec{k}'$ for both frames. This choice for the y axis leads to simpler expressions for the rotation matrices that connect the angular momentum states in the two frames. In this case the initial and final photons have well-defined projections of angular momentum or helicity; thus in Eq. (3) p or $p'=\pm1$ only. In optics, photons with positive (negative) helicity are defined as left (right) circularly polarized.

The first term in brackets in Eq. (3) corresponds to Thomson scattering $f^T(\vec{Q})=g(Q)+f^{ss}(\vec{Q})$ in nonrelativistic theory, i.e., x-ray scattering by electric charges. The modified form factor $g(Q)$ is spherically averaged and is expressed as a sum over eigenstates j, where $\rho_j^{at}(r)$ is the contribution to the total atomic charge density $\rho^{at}(r)$ from orbital j with energy E_j and potential $V(r)$. This form was found to represent the sum over negative-energy eigenstates quite accurately in comparison with precise scattering matrix calculations.[8] For small momentum transfer and neutral atoms, this term can be approximated to good accuracy for all Z by $g(Q)=f_0(Q)-(Z/82.5)^{2.37}$, where

$$f_0(Q)=\int r^2dr\rho^{at}(r)\sin(Qr)/Qr$$

is the usual atomic form factor. The original estimate by Cromer-Liberman,[1] $g(Q)=f_0(Q)+(5/3)E_{tot}/mc^2$, was found to be less accurate.[2]

The quantity $f^{ss}(\vec{Q})$ is the solid-state contribution to the form factor that arises from the difference between the total electron density including solid-state corrections, and the pure atomic electron density $\delta\rho=\rho-\rho^{at}$, where $\vec{Q}=\vec{k}'-\vec{k}$ is the momentum transfer. Actually this term is zero for the FSA due to charge neutrality, and also becomes small for large Q, where the contribution from valence electrons becomes small. Thus this term is typically small for Bragg peaks and FSA.

The second term in Eq. (3) is the anomalous scattering factor f^A, which is due to the excitation of virtual electron-hole pairs, and is the central quantity of interest in this paper. The calculation of f^A reduces to calculations of $f^A_{pp'}$ and $\overline{f}^A_{p'p}$, in Eq. (3), where Γ_j is the core-hole lifetime for core state j. This factor has a cusp singularity at every absorption edge. Above the edge, XAFS-like solid-state effects modulate the calculated scattering amplitude typically by about 0.5 or more electron units or about 10–20%. Nonisotropic solid-state contributions also lead to several effects absent in purely atomic calculations, such as XNCD and the scattering of initial in-plane polarization photons into final normal-to-plane polarization photons, i.e., XACS. The last term $\overline{f}^A$ gives a very smooth contribution, since it has poles at large (for x-rays) negative frequencies $\omega=E_j-E_f$. Below we develop a general framework for calculations of f^A, applicable for positive and negative ω. Thus $\overline{f}^A$ can be determined from f^A as shown in Eq. (3).

The Thomson term in Eq. (3) has a simple polarization dependence

$$\left[\hat{\epsilon}'^*\cdot\hat{\epsilon}=\sum(\epsilon'_{p'})^*r^1_{p'p}(2\theta)\epsilon_p\right],$$

where θ is the Bragg scattering angle and $r^{l}_{p'p}(2\theta)$ is the rotation matrix.[11] This expression simplifies for linear initial and final polarizations. To this end, one defines a polarization vector $\vec{\sigma}=\hat{k}\times\hat{k}'$ normal to the scattering plane, and vectors $\vec{\pi}=\hat{\sigma}\times\hat{k}$ and $\vec{\pi}'=\hat{\sigma}\times\hat{k}'$. Then one can obtain a complete description of polarization dependence in terms of a 2×2 matrix $F_{\alpha\beta}$ defined for each value of ω, $\hat{k}$, and $\hat{k}'$, which is sufficient to obtain the amplitude for any experimental arrangement of initial and final polarizations including phase shifts introduced by polarizers, quarter-wave plates, etc, i.e.,

$$f(\omega,\hat{k}',\hat{\epsilon}',\hat{k},\hat{\epsilon})=\begin{pmatrix}\epsilon'_\sigma\\ \epsilon'_\pi\end{pmatrix}^{\dagger}\begin{pmatrix}F_{\sigma\sigma} & F_{\sigma\pi}\\ F_{\pi\sigma} & F_{\pi\pi}\end{pmatrix}\begin{pmatrix}\epsilon_\sigma\\ \epsilon_\pi\end{pmatrix}. \quad (4)$$

Note that the Thomson term cannot contribute to the cross term, since $\hat{\epsilon}'^{*}\cdot\hat{\epsilon}=0$. For spherically symmetric scatterers the second term (anomalous scattering) also gives zero for the cross term (see discussion of Hönl theory below). However, the cross terms may become nonzero due to solid-state effects. The connection between rectilinear and circular polarizations can be obtained from the transformation[11,12]

$$\begin{pmatrix}\epsilon_+\\ \epsilon_-\end{pmatrix}=\frac{1}{\sqrt{2}}\begin{pmatrix}-i & -1\\ -i & +1\end{pmatrix}\begin{pmatrix}\epsilon_\sigma\\ \epsilon_\pi\end{pmatrix}. \quad (5)$$

This gives the matrix elements of F as

$$\begin{aligned}F_{\sigma\sigma}&=(F_{++}+F_{+-}+F_{-+}+F_{--})/2,\\ F_{\sigma\pi}&=-i(F_{++}-F_{+-}+F_{-+}-F_{--})/2,\\ F_{\pi\sigma}&=i(F_{++}+F_{+-}-F_{-+}-F_{--})/2,\\ F_{\pi\pi}&=(F_{++}-F_{+-}-F_{-+}+F_{--})/2,\\ F_{p'p}&=f^{T}(\vec{Q})r^{1}_{p'p}(2\theta)+f^{A}_{p'p}+\overline{f}^{A}_{p'p}.\end{aligned} \quad (6)$$

Within the RSGF method one calculates the retarded $(-)$ and advanced $(+)$ Green's function $G^{\pm}$ in position space using MS theory,[6] where $G^{\pm}$ has the spectral representation,

$$G^{\pm}(\vec{r},\vec{r}',E)=-\sum_{i}^{\text{all}}\frac{\phi_i^{*}(\vec{r})\,\phi_i(\vec{r}')}{E_i-E\pm i\,\eta}. \quad (7)$$

Below we need G^{+} in the lower half of the complex E plane and G^{-} in the upper half-plane. By exploiting their analyticity in the corresponding half-planes, one gets one from the other using the relationship $G^{+}(E^{*})=G^{-}(E)^{\dagger}$, which can be obtained from Eq. (7).

In order to evaluate the anomalous scattering amplitude it is convenient to calculate certain energy dependent Green's function matrix elements $\hat{G}^{\pm}_{p'p}(E)$ defined as

$$\hat{G}^{\pm}_{p'p}(E)=\langle j|\alpha^{\dagger}_{p'}e^{-i\vec{k}'\cdot\vec{r}'}G^{\pm}(\vec{r}',\vec{r},E)\,\alpha_p e^{i\vec{k}\cdot\vec{r}}|j\rangle. \quad (8)$$

To introduce the finite temperature Fermi function f_T and core-hole lifetime Γ effects, we proceed as follows. First, one can replace the sum over unoccupied states by the integral of the spectral density function

$$A(\vec{r}',\vec{r},E)=(G^{+}-G^{-})/(2\pi i)=\sum_{j}^{\text{all}}\phi_j^{*}(\vec{r}')\,\phi_j(\vec{r})\,\delta(E-E_j)$$

over the Fermi distribution. Second, the complex x-ray scattering amplitude $f^{A}_{p'p}$ is separated into a sum over contributions from individual absorption edges j:

$$f^{A}=\sum_{j}f^{A}_{j},$$

where for a given j,

$$f^{A}_{p',p}(\omega)=\sum_{j}\int_{-\infty}^{\infty}dE\times\frac{1-f_T(E-\mu)}{E_j-E+\omega+i\Gamma_j}\,\frac{\hat{G}^{+}_{p',p}(E)-\hat{G}^{-}_{p',p}(E)}{2\pi i}. \quad (9)$$

This is a general expression and can be implemented in any electronic structure method. However in order to obtain f^{A} accurately to within a few percent, the integration range can go as high as 70 000 eV.[1] This high limit for the energy integration puts a severe limitation on applicable electronic structure methods. Remarkably, the real-space multiple-scattering theory is still applicable, especially since at high energies the fine structure becomes negligible and hence only the first term in the MS series [see Eq. (10) below], i.e., the central embedded atomic contribution, needs to be calculated.

Within MS theory and spherical muffin-tin potentials, $G^{\pm}(E)$ is separable in terms of regular R_κ and irregular H_κ solutions of the Dirac equation at energy E above the muffin-tin zero level (or interstitial potential) in an angular momentum $K=(\kappa,m_j)$ basis:

$$G^{-}(\vec{r},\vec{r}',E)=G^{at}+G^{sc}, \quad (10)$$

$$G^{at}=-\sqrt{8E}\sum_{K}\chi_K R_\kappa(r_<)H_\kappa(r_>)\chi^{\dagger}_K,$$

$$G^{sc}=-\sqrt{8E}\sum_{K,K'}\chi_K R_\kappa(r)e^{i(\delta_\kappa+\delta_{\kappa'})}G^{sc}_{K,K'}R_{\kappa'}(r')\chi^{\dagger}_{K'},$$

$$G^{sc}_{K,K'}=i^{l-l'}\langle J|LS\rangle G^{sc}_{LS,L'S'}\langle L'S'|J'\rangle,$$

where χ_K is the Dirac spinor, and the last equation is a transformation from relativistic K to nonrelativistic LS basis using Clebsh-Gordon coefficients. Here G^{sc} is calculated using the dimensionless Rehr-Albers definitions and sign conventions[13] in a LS basis; this needs to be mentioned to avoid minus sign problems, since different authors define the terms differently. Similarly the expression for G^{+} can be obtained from $(G^{-})^{\dagger}$. With the above representation, we never have to keep G as a function of two space variables, and it is more efficient to store just the regular and irregular solutions. For the central atom part it suffices to carry out calculations for real energies. Then the irregular solution does not enter any of the results, since it cancels in the com-

bination $G^+ - G^-$. Using the multipole expansion for the interaction with the electromagnetic field,[12] we obtain

$$G^-_{p'p}(E) = \sum_{K,m}^{\text{all}} (-)^{j-j'+l_2'+1} R^{l_2' l_2}_{\kappa'} (-p')^{l_2+l_2'+1} \times \begin{pmatrix} j' & l_2 & i \\ -m_j' & p' & m_i' \end{pmatrix} G_{K',K''} r^{j}_{m_j'', m_j} \times (2\theta)(-p)^{l_1+l_1'+1} \begin{pmatrix} j & l_1 & i \\ -m_j & p & m_i \end{pmatrix} r^{i}_{-m_i', -m_i} \times (2\theta) R^{l_1' l_1}_{\kappa}, \tag{11}$$

$$G^+_{pp'}(E^*) = [G^-_{pp'}(E)]^\dagger = G^-_{p'p}(E)^*, \tag{12}$$

where $j'' = j$. A detailed expression for the multipole matrix elements $R^{l'l}_{\kappa}$ is given in the Appendix. Equation (12) shows that we don't need separate subroutines to calculate G^+, since we only need G^+ in the lower-half of the complex energy plane and G^- in the upper-half plane. For the scattering contribution, calculations are carried out in the complex E plane. In contrast to the behavior of the central atom contribution, the scattering part is not smoothly varying for real energies. Indeed for finite molecules it should have δ function singularities at the position of every molecular bound state as well as XAFS-like fine structure in the continuum. The difficulty of handling such rapidly varying structure can be overcome by introducing a finite imaginary part. Therefore we treat separately the embedded atom and solid-state contribution to the elastic-scattering amplitude.

Using the expression for the direct product of two rotation matrices given by Messiah's Eq. (C. 69),[11] one can perform the summation over angular momenta projections m_i and m_j, and obtain

$$G^-_{p'p}(E) = \sum_{K,m}^{\text{all}} (-)^{j-j'+m+l_2'} R^{l_2' l_2}_{\kappa'} \times (-p')^{l_2+l_2'+1} \begin{pmatrix} j' & l_2 & i \\ -m_j' & p' & m_i' \end{pmatrix} \times G_{K',K''} \begin{pmatrix} j & l_1 & i \\ -m_j'' & m & m_i' \end{pmatrix} r^{l_1}_{m,p} \times (2\theta) R^{l_1' l_1}_{\kappa} (-p)^{l_1+l_1'+1}. \tag{13}$$

The central atom contribution can be further simplified, since it is proportional to $\delta_{K,K'}$. More generally the Green's function is diagonal with respect to K for the cases of spherical symmetry or a polycrystalline average in nonmagnetic materials. Thus the polycrystalline average in nonmagnetic systems can be achieved within the RSGF method by the replacement:

$$G_{L,L'} \to \frac{\delta_{L,L'}}{2l+1} \mathrm{Tr}_m G_{L,L}, \tag{14}$$

i.e., by performing trace over the projection of angular momentum for each angular momentum component $L=(l,m)$ separately. The sum over m and m_s leads to a Green's function diagonal also in the K basis $G_{K,K'} = G_0 \delta_{K,K'}$. After summation over m_i', m_j', and m_j'':

$$G^-_{p'p}(\hat{k},\hat{k}',E) = \sum_{\kappa l' l} (-)^{l'+1} (R^{l'l}_{\kappa})^2 (pp')^{l+l'+1} r^{l}_{p'p}(2\theta) \frac{G_0}{2l+1} = \sum_{\kappa l} (-)^{l} [(R^{El}_{\kappa})^2 - (R^{Ml}_{\kappa})^2 pp'] r^{l}_{p'p}(2\theta) \frac{G_0}{2l+1}. \tag{15}$$

Notice that all cross terms, e.g., dipole-quadrupole, cancel out in this case. Also, all angular dependence is contained in the rotation matrix $r^{l}_{p'p}(2\theta)$ and is energy independent. Substituting the explicit expression for the rotation matrix[11] and using Eq. (14) we recover the very compact Hönl theory for the angular polarization dependence of the elastic-scattering amplitude.[14]

$$F_{\sigma\pi} = F_{\pi\sigma} = 0, \tag{16}$$

$$F_{\sigma\sigma} = f^T(\vec{Q}) + f^A_{E1} + [f^A_{E2} + f^A_{M1}]\cos(2\theta),$$

$$F_{\pi\pi} = [f^T(\vec{Q}) + f^A_{E1}]\cos(2\theta) + f^A_{E2}\cos(4\theta) + f^A_{M1},$$

where f_{El} are the electric dipole and quadrupole contributions to the elastic forward-scattering amplitude. Note too that the magnetic dipole contribution (f_{M1}) has a different angular dependence than the electric dipole (f_{E1}), which is a consequence of additional polarization dependence due to the multiplier pp' for the Ml terms. In the case when a fraction q of the incoming radiation has in-plane polarization, the scattered intensity is $I = q|F_{\pi\pi}|^2 + (1-q)|F_{\sigma\sigma}|^2$. The quadrupole and magnetic dipole contributions have different angular dependencies than the electric dipole contribution; however, this might be difficult to single out experimentally, since $f^T(\vec{Q})$ is also angular dependent, and the energy dependence will be dominated by that of the electric dipole contribution.

III. COMPLEX ENERGY PLANE CALCULATION OF G^{sc}

Equation (9) above is formally similar to a Kramers Kronig transform of the absorption coefficient, however we now modify it, using the analyticity of $\hat{G}(E)$ in the complex E plane. As noted above, it is sufficient to carry out the manipulations for G^- in the upper half E plane. We will assume that the temperature is smaller than the core-hole lifetime broadening ($2\pi k_B T < \Gamma_i$), which is usually a good assumption since Γ/k_B usually exceeds 2000 K (i.e., about 0.2 eV). We also treat separately the contributions from the advanced and retarded Green's functions: $f_{pp'} = f^+_{pp'} + f^-_{pp'}$ for each edge j. Using periodicity of f_T in imaginary E, we shift the integration into the complex E plane by $2\pi ikT$, yielding

$$f^{-}_{pp'}(\omega)=\frac{-1}{2\pi i}\sum_j \int_{-\infty+2\omega_1}^{\infty+2\omega_1} dE \frac{\hat{G}^{-}_{pp'}(E)[1-f_T(E-\mu)]}{E_j-E+\omega+i\Gamma_j} + kT\frac{\hat{G}(\mu+w_1)}{E_j-\mu-w_1+\omega+i\Gamma_j}, \quad (17)$$

where the last term corresponds to the contribution from the first Matsubara pole located at $E=\mu+w_1$ and $w_1=i\pi kT$.

On the real axis the integrand can have sharp singularities due to band structure or bound states. Here, due to the addition of a finite imaginary part, the integrand is a much smoother function. Hence one can safely approximate the integral by the first term of the Sommerfeld expansion and eliminate the Fermi-Dirac distribution. In the following we focus attention on the contribution from a given edge j and suppress the subscripts p,p' and superscript $(-)$.

$$f_j(\omega)=\int_{\mu+i2\pi kT}^{\infty+i2\pi kT} dE\frac{\hat{G}(E)}{E_j-E+\omega+i\Gamma_j} + \left[kT\frac{\hat{G}(\mu+w_1)}{E_j-\mu-w_1+\omega+i\Gamma_j} + \frac{iw_1^2}{12\pi}\frac{d}{dE}\left(\frac{\hat{G}(E)}{E_j-E+\omega+i\Gamma_j}\right)\right]. \quad (18)$$

The terms in square brackets correspond to a Sommerfeld correction of order kT and contributions from the Matsubara pole(s), both of which are comparable in order of magnitude. In the expressions below, they will be denoted as $\delta f_j(T)$, but they can generally be neglected. If the validity of Sommerfeld expansion is in doubt, due to the smallness of kT, the contour may be shifted several times, i.e., by $ni2\pi kT$, yielding contributions from n Matsubara poles and a much more smoothly varying integrand that can be safely treated with the Sommerfeld expansion.[15] Finally, we change the integration contour to the imaginary axis by closing the contour at infinite radius, yielding

$$f_j(\omega)=\theta(\omega-E_j+\mu)\hat{G}(\omega-E_j+i\Gamma_j)+\delta f_j(T) - \frac{1}{2\pi i}\int_{\mu+2w_1}^{\mu+i\infty} dE\frac{\hat{G}(E)}{E_j-E+\omega+i\Gamma_j}. \quad (19)$$

Notice that the first term, which comes from the core-hole pole, contains all the fine structure above the Fermi level. Although not indicated explicitly, it is straightforward to include correlated Debye-Waller factors and structural disorder in $\hat{G}$, as in the FEFF8 code.[6] The θ function zero-temperature Fermi prefactor might suggest that f_i has a jump at Fermi level. However, this jump is exactly canceled by an opposite jump from the integral when the core-hole pole crosses the imaginary integration contour. Thus all features in f_j are actually broadened by the core-hole lifetime plus a contribution from the imaginary part of the final-state self-energy which vanishes at the edge. Note that without the core-hole lifetime and thermal broadening, f' would have a logarithmic singularity at the Fermi energy. We remark that the above expression could be modified to avoid the apparent jumps at Fermi level by adding and subtracting in the numerator of the integrand a term proportional to $G(\mu+i\Gamma)$ times a single-pole function, which is equal to one for $E=\mu+i\Gamma$, and which has a pole in the lower half-plane, but this would not change the result.

IV. APPLICATIONS

The relativistic approach outlined above is quite general and is also applicable for calculations of elastic scattering even in magnetic materials. Indeed, it would be interesting to apply the method to studies of the DAFS of Bragg peaks in magnetic materials. However for simplicity in the present paper, we demonstrate the approach for less complicated cases, e.g., DAFS, XNCD, and XACS. All calculations were carried out for the special case of forward scattering ($\vec{Q}=0$), but the generalization to arbitrary $\vec{Q}$ is straightforward and can be done using Hönl theory in many cases. Traditionally the Rayleigh scattering amplitude is separated as $f=f_0(Q)+f'(E)+if''(E)$, i.e., using the atomic form factor and with the transfer of the relativistic correction in the Thomson term [g(Q)] into the anomalous scattering amplitude: $f'=f^A+\overline{f^A}-(Z/82.5)^{2.37}$. In our view it is more natural to add this correction to the Thomson term [$g(Q)$ is the modified form factor], but for comparison with other calculations and experiment we follow the above convention for f'.

The theory described above has been implemented in a computer code FEFF8.10, which is a generalization of the *ab initio*, self-consistent FEFF8 code[6] and uses the same potentials, phase shifts, and other fundamental ingredients. We use the general expression in Eq. (11) to calculate $G^{-}_{pp'}$ in the complex energy plane, with $G_{K,K'}$ given by Eq. (10) and multipole matrix elements given in the appendix. We perform separate calculations for the central atom part and for the scattering part as outlined above. The embedded atom calculations are similar to those of Cromer-Liberman, but are carried out for the central atom embedded in a solid rather than a free atom, and also include the core-hole lifetime. Thus the embedded atom potential is weakly sensitive to the environment and can exhibit some solid-state effects like atomic XAFS.[7] We calculate absorption coefficients up to very high energies and use Eq. (17) to get the embedded atom contribution to f'. The scattering contribution decays rapidly at high energies and thus needs to be calculated relatively close to the edge (the EXAFS region extends at most 2000 eV). The solid-state contribution to the anomalous scattering amplitude (real and imaginary parts) is obtained using Eq. (19), i.e., using the values of $\hat{G}$ on imaginary axis.

The calculations of f' and f'' with FEFF8.10 are compared with recent results from atomic theory in Table I, for energies far from the edges where solid-state effects are negligible. Indeed our results come only from the embedded atom contributions. Table I also illustrates the good agreement between all of these atomic calculations and experiment. We remark that to get this agreement, quadrupole terms had to be included. Otherwise the calculated absorption coefficient at high energies is too small. The Cromer-Liberman and Kissel *et al.* results are comparable, since a relativistic Dirac-Fock-Slater code was used in both cases, while our calculations were performed with the relativistic Dirac-Fock code. We

TABLE I. Comparison of f' and f'' for noble gases between various calculations and theory. The experimental and Cromer Liberman (CL) results are taken from Ref. 1. The CL f' results were corrected to obtain a better $f_0{}^2$ (see text); the Kissel *et al.* results were obtained using their program, which is available on the WWW (Ref. 2).

Atom	Expt.	Present	CL	Kissel
Ne f'	−0.01	0.027	0.026	0.026
Ar f'	0.10	0.181	0.175	0.176
Kr f'	−0.81	−.540	−.545	−.533
Ne f''	0.017(4)	0.016	0.02	0.017
Ar f''	0.202(5)	0.201	0.201	0.203
Kr f''	2.78(7)	2.70	2.71	2.71

have included in the Cromer-Liberman results reported here a correction that gives an improved contribution from negative-energy states.[2]

A. Anomalous scattering amplitude f' for Cu

The scattering contribution is greatly simplified for nonmagnetic, polycrystalline samples or for materials with cubic symmetry. The angular dependence in this case is given by Hönl theory, Eq. (16), where anomalous scattering needs to be calculated explicitly only for the forward-scattering amplitude. However the solid-state effect on diagonal terms $F_{\sigma\sigma}$ and $F_{\pi\pi}$ is not negligible near an edge. We calculated f' using only the dipole approximation for the scattering part and up to quadrupole contributions for the embedded atom part. Calculations for the Cu K edge anomalous scattering amplitude f' using FEFF8.10 are compared to experiment in Fig. 1. The experimental curve for f' has been derived from the energy dependence of the Bragg peak intensity using the iterative DKK approach.[3] One clearly sees that solid-state effects are quite important near the edge. The agreement with experiment is remarkable and shows that quantitative agreement for the scattering amplitude, even in the region where solid-state effects are non-negligible, is possible. Although fcc Cu metal is one of the simplest structures, it has large solid-state effects and hence serves well as a test case. For more complicated systems the inclusion of nonspherical parts of the potential and possibly many-body corrections may also be necessary.

To show the importance of subtracting the contribution from states below Fermi level, we also performed calculations where such subtractions were neglected (short dashes in Fig. 1). This result shows a strong deviation from the experimental curve at the edge, and the difference only becomes negligible about 100 eV above the edge.

B. Cross terms $F_{\sigma\pi}$ and $F_{\pi\sigma}$

In the near-edge region where solid-state effects are important, quadrupole transitions are usually small compared to the dipole terms. Thus one may use the above polycrystalline expression for the central atom contribution and the dipole approximation for the scattering part of the Green function. Therefore all angular dependence will be of the form $\boldsymbol{\epsilon}_i f^{sc}_{i,j} \boldsymbol{\epsilon}'_j$. For nonmagnetic materials, real polarizations can be chosen. For crystals with symmetry axes of more than three-dimensional 3D order, f^{sc} will be diagonal when the z axis is along the symmetry axis. For uniaxial crystals $f^{sc}_z \neq f^{sc}_x = f^{sc}_y$, we have $\boldsymbol{\epsilon}_i f^{sc}_{i,j} \boldsymbol{\epsilon}'_j = f^{sc}_x \boldsymbol{\epsilon}_i \boldsymbol{\epsilon}'_i + (f^{sc}_z - f^{sc}_x)\boldsymbol{\epsilon}_z \boldsymbol{\epsilon}'_z$ and

$$F_{\sigma\sigma} = f^T(\vec{Q}) + f^{sc}_x + (f^{sc}_z - f^{sc}_x)(\sigma_z)^2, \tag{20}$$

$$F_{\sigma\pi} = (f^{sc}_z - f^{sc}_x)\sigma_z \pi_z,$$

$$F_{\pi\sigma} = (f^{sc}_z - f^{sc}_x)\sigma_z \pi'_z,$$

$$F_{\pi\pi} = [f^T(\vec{Q}) + f^{sc}_x]\cos(2\theta) + \pi_z \pi'_z (f^{sc}_z - f^{sc}_x).$$

Note that due to solid-state effects, the cross term does not cancel out, unless the z axis is normal to either initial or final polarizations. Thus the cross terms are sensitive only to solid-state effects. As an example we present calculations for the hcp Cd metal. In Fig. 2 we show the calculated $|(f^{sc}_z - f^{sc}_x)|^2$ versus both calculated and experimental[18] absorption coefficients for in-plane (x,y) polarization. Clearly our x-ray

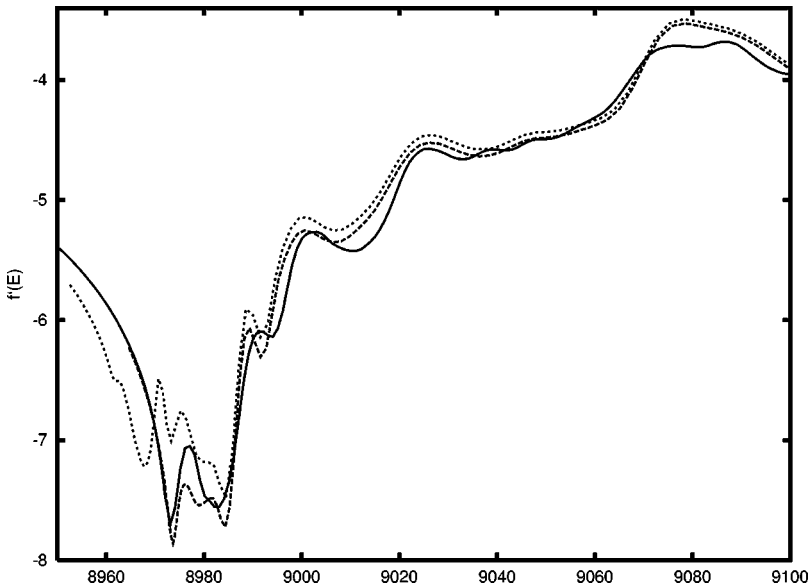

FIG. 1. Calculated (dashes) and experimental (Ref. 3) (solid) anomalous scattering amplitude (f') near the Cu K edge. Calculation with (long dashes) and without (short dashes) subtraction of states below Fermi level.

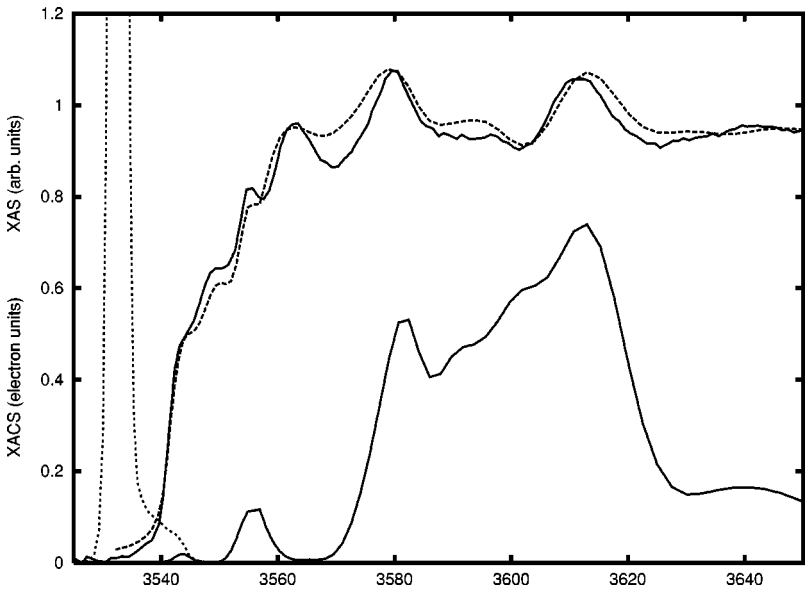

FIG. 2. Calculated (dashes) and experimental (Ref. 18) (solid) Cd L_3 edge absorption (XAS) for polarization parallel to Cd hcp plane show good agreement. The XACS $|F_{\pi\sigma}|^2$ is nonzero due to solid-state effect. Calculations without subtraction of states below the Fermi level are shown by dots.

absorption calculations are in good agreement with experiment. Notice that for each peak in the cross term scattering there are roughly two peaks in absorption.

We also show (Fig. 2 dots) results of calculations carried out without subtracting the contribution from the states below the Fermi level, i.e., at about 3541 eV. The big peak (dots) just below Fermi level corresponds to the band of $4d$ states, which are completely occupied for Cd. Thus one expects an even stronger effect on the spectra near the Fermi level in cases when the d states are partially occupied (e.g., for transition metals). However, we do not present such calculations here, as such materials are often magnetic and we plan to address the generalization to spin dependent systems in future work. Previous MS calculations[9,16] did not address the problem of subtracting the contribution from the states below Fermi level. For example, one obtains a similar result for the forbidden Bragg scattering in $LaMnO_3$.[16] The importance of such subtractions for the cross term is small for $LaMnO_3$ since the Fermi level is within a band gap. However this subtraction is essential for the diagonal terms, for which there is a large sensitivity of the cusp intensity to the position of Fermi level (Fig. 1). As indicated above, a bigger effect of subtraction on the cross term can be expected for magnetic metals and cannot be totally neglected even for Cd.

C. X-ray natural circular dichroism

The effect of XNCD observed in nonmagnetic materials can originate from the cross dipole-quadrupole ($E1$-$E2$) transitions or even in dipole approximation due to nonlinear wave propagation.[17] Our general expression for $G(E)$ simplifies for forward scattering ($\theta=0$), since the rotation matrices then become unit matrices. Only gyrotropic XNCD is possible in the $LiIO_3$ crystal, and for the propagation along the symmetry axis one has from the optical theorem,

$$\sigma_{XNCD}=\sigma_+-\sigma_-=\mathrm{Im}\frac{4\pi}{\omega c}(f^A_{++}-f^A_{--}). \tag{21}$$

The XNCD at the I L_3 edge is shown in Fig. 3. Our calculations generally agree both with experiment and with previous results for the overall peak positions and intensities.

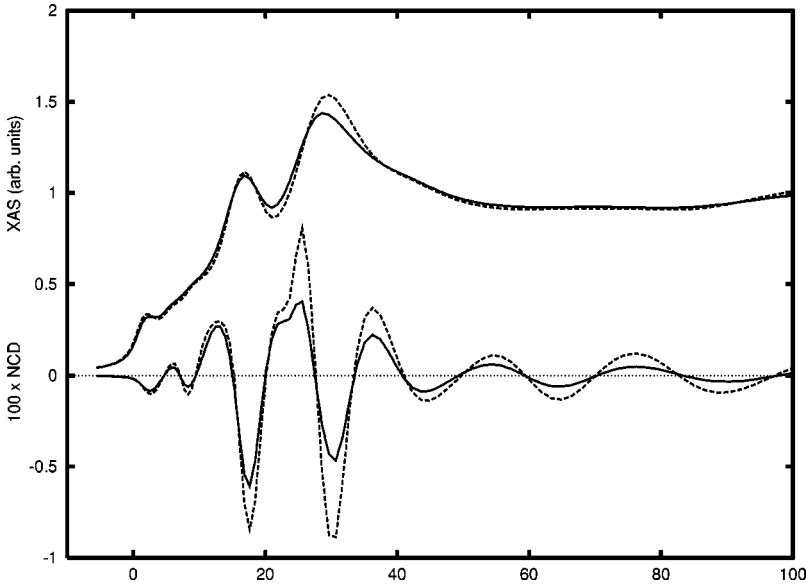

FIG. 3. Calculated XAS (upper) and XNCD (lower) for iodine L_3 edge in LiIO3 with Debye-Waller factors (solid) and without (dashes). The XNCD signal is multiplied by 100. XNCD vanishes for spherically symmetric potentials and thus is due entirely to solid-state effects.

However some details of our results are somewhat different since, in contrast to previous calculations,[16] our code is relativistic and self-consistent and also includes the damping effects of Debye-Waller factors. Moreover, we do not agree with the conclusion[16] that convergence can be achieved with a 40 atom cluster. Clearly Fig. 3 shows noticeable changes for a 101 atom cluster, especially for XNCD. However, we find that increasing the size beyond 101 atoms, e.g., to 149 atoms gives little further change. Also note that our calculations correctly reproduce the negative XNCD peak at the same position as the first absorption peak—about 1 eV above the edge, which was not reproduced correctly previously. We also show in Fig. 3 the effect of Debye-Waller factors, which shows that thermal disorder is a primary source of the overestimated amplitude in earlier calculations.

For all calculations it is surprising that agreement with experiment is better for XNCD than for absorption.[19] The source of the discrepancies may be due to the limitations of muffin-tin potential used in all of the calculations and possibly to multielectron excitations, as suggested by Natoli. In our view, the nonspherical part of the potential may strongly affect x-ray appearance new-edge structure (XANES) calculations and its role for XANES and XNCD needs to be addressed quantitatively in future work.

V. CONCLUSIONS

We have developed a general theoretical approach for calculations of the x-ray elastic scattering amplitude, including solid-state effects within the RSGF formalism. In this approach, calculations of f' and f'' are carried out simultaneously in the complex E plane, without the necessity of the DKK transformation. The theory is implemented in a generalization of the *ab initio* x-ray spectroscopy code FEFF8.10 which is applicable to arbitrary materials. This generalization extends the capabilities of FEFF8 to treat a number of x-ray spectroscopies and also extends the domain of validity to very-high energies. In our approach, calculations are carried out separately for the atomiclike and solid-state parts, since their corresponding contributions to the Green's function have different behaviors for large complex energies. The solid-state effect is particularly significant for Bragg-peak intensities for energies near the absorption edge (DAFS). Purely solid-state effects can be observed by measuring the XACS term $F_{\sigma\pi}$ or XNCD. Calculations of these effects with the same RSGF method in FEFF8.10 show good agreement with experiment. Near the absorption edge we find that it is important to account for finite core-hole lifetime and to subtract the contribution from occupied states. For nonmagnetic materials this seems to be most important for the diagonal terms $F_{\sigma\sigma}$ and $F_{\pi\pi}$. Far from the edge, in the extended fine-structure region, the contribution from states below the edge can be neglected. This implies that calculations of DAFS can be simplified, in that the terms arising from the subtraction of occupied states, i.e., from the integral over the imaginary axis in Eq. (19) can be neglected. This integral is essential to obtain an accurate treatment of the cusp, but its behavior is smooth both above and below the Fermi level. A similar RSGF formalism is applicable to other spectroscopies, such as reflectivity fine structure, or nonresonant x-ray emission spectra (XES), and we plan to address these topics in future work.

ACKNOWLEDGMENTS

We are grateful to C. Brouder, J. O. Cross, L. Kissel, M. Newville, R. Pratt, and R. Vedrinskii for useful comments and to D. Chandesris for experimental Cd data. This work was supported in part by US DOE Grant No. DE-FG03-97ER45623.

APPENDIX

Below we summarize the details of the calculation of multipole matrix elements used in this work. Following the review and notation of Grant,[12] we consider the fully relativistic expression for matrix elements of multipole transitions:

$$\langle n\kappa m|\alpha_p e^{i\vec{k}\cdot\vec{r}}|n'\kappa' m'\rangle. \tag{A1}$$

The quantum number $\kappa=l$ for $j=l-1/2$, and $\kappa=-l-1$ for $j=l+1/2$. Expressions for the matrix elements can be obtained using irreducible tensor algebra,[11,20] using the decomposition of $e^{i\vec{k}\cdot\vec{r}}$ in terms of the irreducible tensors $C_0^{(l')}$. The vector operator $\vec{\alpha}$ is a tensor of order 1. The product of two tensors can be decomposed in terms of the irreducible tensors,[11,20]

$$\alpha_p e^{i\vec{k}\vec{r}}=\sum_{l=1}^{\infty}\sum_{l'=l-1}^{l+1} a_{l'l}\begin{pmatrix} 0 & X_p^{[(l'1)l]} \\ X_p^{[(l'1)l]} & 0 \end{pmatrix}(-p)^n, \tag{A2}$$

where $n=l'+l+1$, and the quantity

$$a_{l'l}(r)=(-)^{l+1}[l]^{1/2}i^{l'}\begin{pmatrix} l & 1 & l \\ 0 & 1 & -1 \end{pmatrix} j_{l'}(kr)(2l'+1), \tag{A3}$$

depends only on r and not on angular or spin coordinates. Conversely the irreducible tensor $X_p^{[(l'1)l]}$ is independent of r and acts on the angular and spin coordinates only. Here the usual notation of atomic physics is used: $[k,l,\ldots]=(2k+1)(2l+1)\ldots$. Thus this operator connects two upper components of the initial-state Dirac spinor only with the two lower components of final-state spinor (and vice versa). Grant's result[12] Eq. (6.30) can be rewritten in a form resembling the Wigner-Eckart theorem:

$$\begin{aligned}\langle n\kappa m|a_{l'l}(r)&\begin{pmatrix} 0 & X_p^{[(l'1)l]} \\ X_p^{[(l'1)l]} & 0 \end{pmatrix}|n'\kappa' m'\rangle \\ &=(-1)^{j-m}\begin{pmatrix} j & l & j' \\ -m & p & m' \end{pmatrix} R_{\kappa\kappa'}^{l'l},\end{aligned} \tag{A4}$$

where the reduced matrix element $R_{\kappa\kappa'}^{l'l}$ is

$$\begin{aligned}R_{\kappa\kappa'}^{l'l}&=\sum_{\beta}\langle n\kappa\beta|a_{l'l}(r)|n'\kappa'-\beta\rangle C_{\kappa\kappa'}^{l'l}(\beta) \\ &=i\int dr\, a_{l'l}(kr)[P_\kappa Q_{\kappa'} C_{\kappa\kappa'}^{l'l}(1)+Q_\kappa P_{\kappa'} C_{\kappa\kappa'}^{l'l}(-1)] \\ &=\int dr\, R_{\kappa\kappa'}^{l'l}(r).\end{aligned} \tag{A5}$$

Here $\beta=\pm 1$ corresponds to the upper (lower) component of Dirac spinor, and

$$C^{l'l}_{\kappa\kappa'}(\beta)=\sqrt{6}[j,l,j',\lambda,\lambda']^{1/2}(-1)^{\lambda}\begin{Bmatrix}\lambda & l' & \lambda'\\ \frac{1}{2} & \frac{1}{2} & 1\\ j & j' & l\end{Bmatrix}\times\begin{pmatrix}\lambda & l' & \lambda'\\ 0 & 0 & 0\end{pmatrix}\delta\left(\lambda,j-\frac{1}{2}a\beta\right)\times\delta\left(\lambda',j'+\frac{1}{2}a'\beta\right), \tag{A6}$$

where the $a=1$ for negative κ and $a=-1$ for positive κ. In the above expression we correct the minus sign problem in Grant's paper for the arguments inside the Kronecker δ symbols.

It is convenient to define electric and magnetic multipole matrix elements as $R^{El}_{\kappa\kappa'}=R^{l-1l}_{\kappa\kappa'}+R^{l+1l}_{\kappa\kappa'}$ and $R^{Ml}_{\kappa\kappa'}=R^{ll}_{\kappa\kappa'}$. Thus the smooth atomic cross section is given as a sum of multipole electric and magnetic contributions

$$\sigma_{at}(\omega)=\frac{8\pi ck}{\omega}\sum_{k'l}\frac{|R^{El}_{\kappa\kappa'}|^2+|R^{Ml}_{\kappa\kappa'}|^2}{2l+1}. \tag{A7}$$

The factor $(-p)^n$ in Eq. (23) is always unity for electric multipole transition, but alternates in sign for magnetic multipole transitions. This factor is essential to calculate the $E1$-$M1$ contribution to XNCD, which we found to be two orders of magnitude smaller than the $E1$-$E2$ contribution at the I L_3 edge in $LiIO_3$. Also this factor leads to a different angular dependence of the scattering amplitude for spherically symmetric or polycrystalline systems.

An additional complication arises for calculations of $G^{\rm at}$ in the complex energy plane, which are necessary if one wants to avoid singular points at the real energies of the bound states, where $G^{\rm at}$ diverges. One can use complex energy integration as discussed in the text for G^{sc}; however for the central atom part, the irregular solution needs to be calculated in order to exploit the analyticity in the upper half-plane. Thus the expression for the embedded atom contribution is

$$G^{-}_{p'p}(\hat{k},\hat{k}',E)=\sum_{\kappa l}(-)^{l'+1}(pp')^n H^{l'l}_{\kappa\kappa'}\frac{r^{l}_{p'p}(2\theta)}{2l+1}$$

$$H^{l'l}_{\kappa\kappa'}=2\int_0^\infty dr\,R^{l'l}_{\kappa\kappa'}(r)\int_r^\infty dr' H^{l'l}_{\kappa\kappa'}(r'), \tag{A8}$$

where $H^{l'l}_{\kappa\kappa'}(r')$ is defined as the regular counterpart in Eq. (A5). Thus one has to calculate the above double integral instead of squaring the matrix element. This has also been implemented in our code to calculate nonresonant x-ray emission spectra (XES), since in this case, calculations on the real axis is not a good choice for the RSGF method. These results will be published elsewhere, since XES does not have a direct relationship to the elastic-scattering amplitude addressed in the present paper.

[1] D.T. Cromer and D. Liberman, J. Chem. Phys. **53**, 1891 (1970).
[2] L. Kissel and R.H. Pratt, Acta Crystallogr., Sect. A: Found. Crystallogr. **46**, 170 (1990); L. Kissel, B. Zhou, S.C. Roy, S.K. Sen Gupta, and R.H. Pratt, *ibid.* **51**, 271 (1995); http://www-phys.llnl.gov/V_Div/scattering/asf.html
[3] J.O. Cross, M. Newville, J.J. Rehr, L.B. Sorensen, C.E. Bouldin, G. Watson, T. Gouder, G.H. Lander, and M.I. Bell, Phys. Rev. B **58**, 11 215 (1998).
[4] S.M. Heald, H. Chen, and J.M. Tranquada, Phys. Rev. B **38**, 1016 (1988).
[5] R.V. Vedrinskii, V.L. Kraizman, A.A. Novakovich, and V.Sh. Machavariani, J. Phys.: Condens. Matter **5**, 8643 (1993).
[6] A.L. Ankudinov, B. Ravel, J.J. Rehr, and S.D. Conradson, Phys. Rev. B **58**, 7565 (1998).
[7] J.J. Rehr, C.H. Booth, F. Bridges, and S.I. Zabinsky, Phys. Rev. B **49**, 12 347 (1994).
[8] P.P. Kane, L. Kissel, R.H. Pratt, and S.C. Roy, Phys. Rep. **140**, 75 (1986).
[9] R.V. Vedrinskii *et al.*, J. Phys.: Condens. Matter **4**, 6155 (1992).
[10] J. J. Sakurai, *Advanced Quantum Mechanics* (Addison-Wesley, Reading, 1967).
[11] A. Messiah, *Quantum Mechanics* (Interscience, New York, 1961).
[12] I.P. Grant, Adv. Phys. **19**, 747 (1970).
[13] J.J. Rehr and R.C. Albers, Phys. Rev. B **41**, 8139 (1990).
[14] H. Hönl, Ann. Phys. (Leipzig) **18**, 625 (1933); Z. Phys. **84**, 1 (1933); A.C. Hazell, Nature (London) **227**, 269 (1970); H.K. Wagenfeld, Z. Phys. **65**, 437 (1965).
[15] P.J. Braspenning, R. Zeller, A. Lodder, and P.H. Dederichs, Phys. Rev. B **29**, 703 (1984).
[16] M. Benfatto, Y. Joly, and C.R. Natoli, Phys. Rev. Lett. **83**, 636 (1999).
[17] V.Sh. Machavariani, J. Phys.: Condens. Matter **7**, 5151 (1995).
[18] P. LeFevre, H. Magnan, and D. Chandesris, Phys. Rev. B **54**, 2830 (1996).
[19] C.R. Natoli, Ch. Brouder, Ph. Sainctavit, J. Goulon, Ch. Goulon-Ginet, and A. Rogalev, Eur. Phys. J. B **4**, 1 (1998); J. Goulon, Ch. Goulon-Ginet, A. Rogalev, V. Gotte, C. Malgrange, Ch. Brouder, and C.R. Natoli, J. Chem. Phys. **108**, 6394 (1998).
[20] B. R. Judd, *Operator Techniques in Atomic Spectroscopy* (McGraw-Hill, New York, 1963).